Electronic Supplementary Information

Experimental section

Materials: $FeCl_3 \cdot 6H_2O$ (≥ 99.0%), NaOH (≥ 90%), Se powder (99.9%), H_2O_2 (30 wt%), and urea (≥ 96%) were purchased from Aladdin Ltd., Shanghai, China. Concentrated HCl was purchased from Tianjin Fuyu Chemical Reagent Co. Ltd., China. Ti plate (99.9 % pure) was provided by Hongshan District, Wuhan Instrument Surgical Instruments business, and was pretreated in HCl and then cleaned by sonication in water and ethanol for several times to remove surface impurities. All chemicals were used as received. The water used throughout all experiments was purified through a Millipore system.

Synthesis of Fe_2O_3 and Se-Fe_2O_3 on Ti plate: $FeCl_3 \cdot 6H_2O$ (0.81g) and urea (0.18g) were dissolved in 40 mL water under vigorous stirring for 30 min. Then the solution was transferred to a 50 mL Teflon-lined stainless-steel autoclave in which a piece of Ti plate was immersed into the solution. Then the autoclave was sealed and maintained at 100 °C for 8 h in an electric oven. After the autoclave cooled down at room temperature naturally, the Ti plate covered with Fe-precursor was taken out and washed with water and ethanol for several times, followed by drying at 60 ºC. Then the Fe-precursor was annealed at 550 °C in air for 2 h to obtain the Fe_2O_3 nanorod array. To synthesize Se-Fe_2O_3, 0.1g Se powder was placed in the center of front zone in a two-zone furnace, while the resulting Fe_2O_3 was put at the center of back zone. Subsequently, the front zone was heated at 300 °C for 30 min with a heating speed of 1.5 °C min^{-1}, meanwhile, the temperature of the back zone was heated at 400 °C for 30 min with a heating rate of 2 °C min^{-1}. Finally, the furnace was allowed to cool down to room temperature under Ar.

Characterizations: XRD measurements were performed using a RigakuD/MAX 2550 diffractometer with Cu Kα radiation (λ = 1.5418 Å). SEM images were collected on a XL30 ESEM FEG scanning electron microscope at an accelerating voltage of 20 kV. TEM measurements were made on a HITACHI H-8100 electron microscopy (Hitachi, Tokyo, Japan) with an accelerating voltage of 200 kV. XPS measurements were

performed on an ESCALABMK II X-ray photoelectron spectrometer using Mg as the exciting source.ICP-MS analysis was performed on ThermoScientific iCAP6300. The diffuse reflectance UV-vis adsorption spectra were recorded on a spectrophotometer (Shimadazu, UV 3600), with fine $BaSO_4$ powder as reference.

Photoelectrochemical measurements: Photoelectrochemical measurements were performed with a CHI 660E electrochemical analyzer (CH Instruments, Inc., Shanghai) in a standard three-electrode system using Fe_2O_3/Ti or Se-Fe_2O_3/Ti as the working electrode, Pt wire as the counter electrode, and Ag/AgCl as the reference electrode in 1.0 M NaOH. Lighting apparatus used in the experiment is simulated solar light irradiation (100 mW cm^{-2}) (PLS-sxe300/300UV). The potentials reported in this work were calibrated to RHE other than especially explained, using the following equation: E (RHE) = E(Ag/AgCl) + (0.197 + 0.059 × pH) V. Polarization curves were obtained by linear sweep voltammetry with a scan rate of 5 mV s^{-1}. All experiments were carried out at room temperature. IPCE measurements were performed under illumination through monochromatic system, composed of a monochromator (Model: 74125, Newport) and light source (Model 73404, Newport) without external bias in a two-electrode model, with Fe_2O_3/Ti or Se-Fe_2O_3/Ti as the anode and Pt wire as the cathode. The electrochemical impedance spectroscopy (EIS) was measured using a PGSTAT 302N Autolab Potentiostat/Galvanostat (Metrohm) equipped with a frequency-analyzer module (FRA2) with an excitation signal of 10 mV amplitude and frequency range between 100 kHz to 0.1 Hz.

The applied bias photon-to-current efficiency (ABPE) is calculated based on the equation:

$$ABPE = \frac{j_{ph}(1.23 - V_b)}{P_{total}}$$

where V_b is the applied bias vs. RHE, j_{ph} is the photocurrent density at the measured potential, and P_{total} is the power density of incident light (100 mW cm^{-2}).

The IPCE of each sample was measured in 1.0 M NaOH at 1.23 V vs. RHE under monochromatic illumination, which is calculated based on the equation:

$$IPCE(\%) = \frac{1240\, I}{\lambda J_{light}} \times 100\%$$

where I is photocurrent density (mA cm^{-2}), J_{light} is incident light irradiance (mW cm^{-2}), and λ is incident light wavelength (nm).

Mott-Schottky measurements were performed at a frequency of 1000 Hz under dark condition in 1.0 M NaOH. The calculation is based on the equation:

$$\frac{1}{C^2} = \frac{2}{N_D e \varepsilon \varepsilon_0}\left[(E_S - E_{FB}) - \frac{k_B T}{e}\right]$$

where C is the space charge capacitance of the semiconductor, ε is the dielectric constant of Fe_2O_3, ε_0 is the permittivity of vacuum, A is the active area of the photoanode, e is the electronic charge, N_D is the charge carrier concentration, E_s is the applied potential, E_{fb} is the flat band potential, k_B is Boltzmann's constant, and T is the absolute temperature. The charge carrier density is calculated based on the equation:

$$N_D = -\left(\frac{2}{e\varepsilon\varepsilon_0}\right)\left(\frac{d\left(\frac{1}{C^2}\right)}{d(E_S)}\right)^{-1}$$

The charge separation efficiency (η_{sep}) and surface transfer efficiency (η_{trans}) is calculated based on the equation:

$$\eta_{trans} = \frac{J_{H_2O}}{J_{H_2O_2}}$$

$$\eta_{sep} = \frac{J_{H_2O_2}}{J_{max} \times \eta_{abs}}$$

Where J_{H_2O} is the measured photocurrent density, $J_{H_2O_2}$ is the photocurrent density in the presence of H_2O_2, $J_{max}\, is$ the maximum theoretical water oxidation photocurrent density, η_{abs} is the light absorption efficiency.

The band gap is estimated by the equation $(\alpha h\nu)^n = A(h\nu - E_g)$, where hν is the incident photon energy, α is the absorption coefficient, and A is a constant. The value of n is 1/2 for hematite.

The amount of oxygen evolved from the photoanode were measured in air-tight H-cell

with a gas chromatograph (Shimadzu, GC-2014).

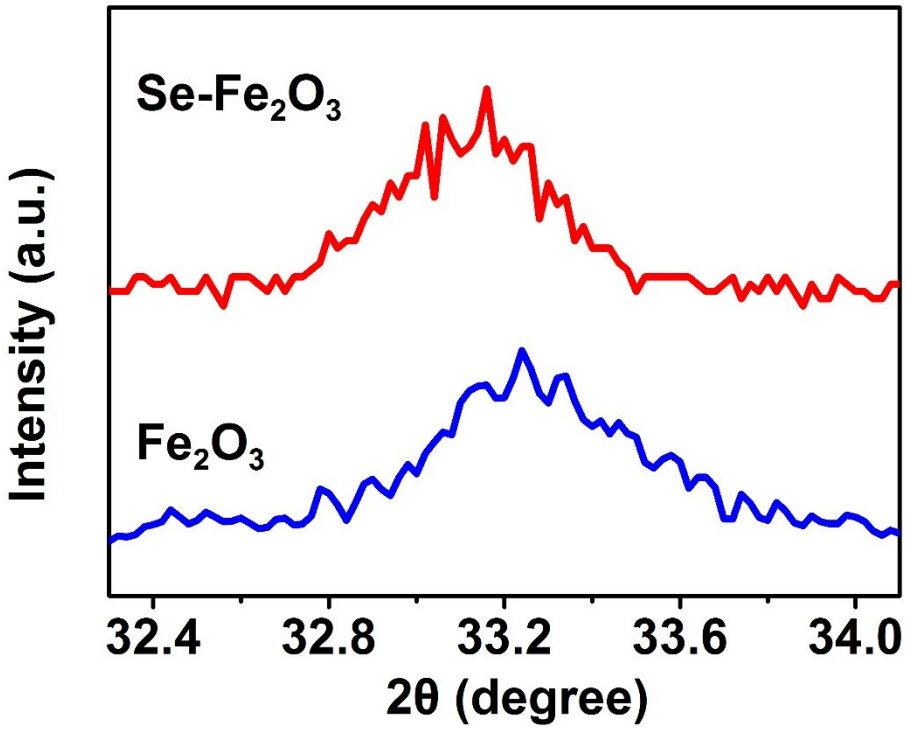

Fig. S1. XRD patterns of Fe_2O_3 and Se-Fe_2O_3 in the (110) plane.

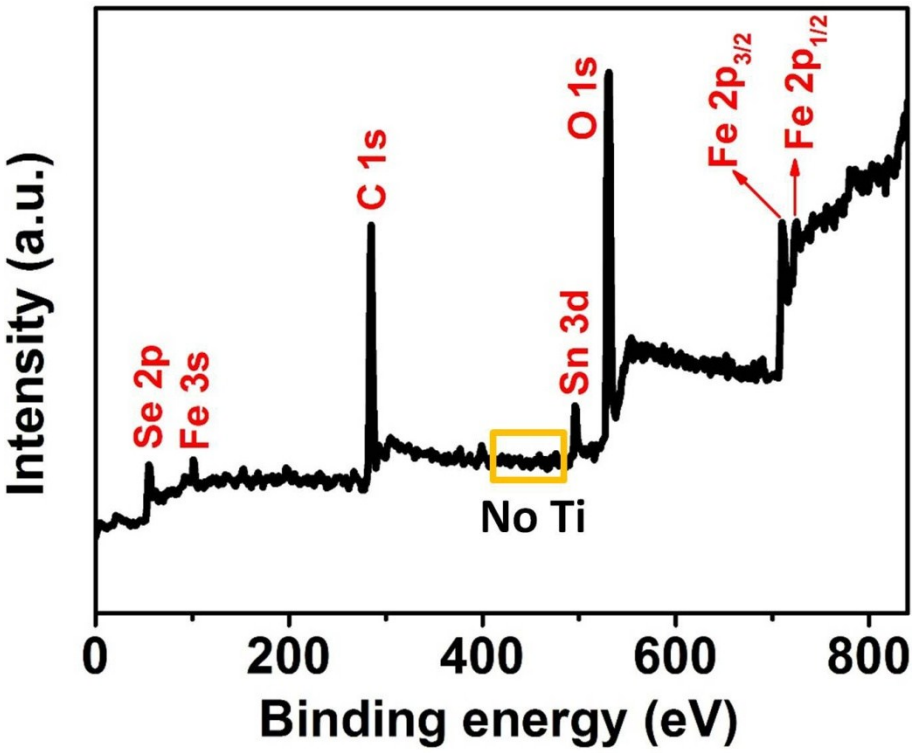

Fig. S2. XPS survey spectrum of Se-Fe_2O_3.

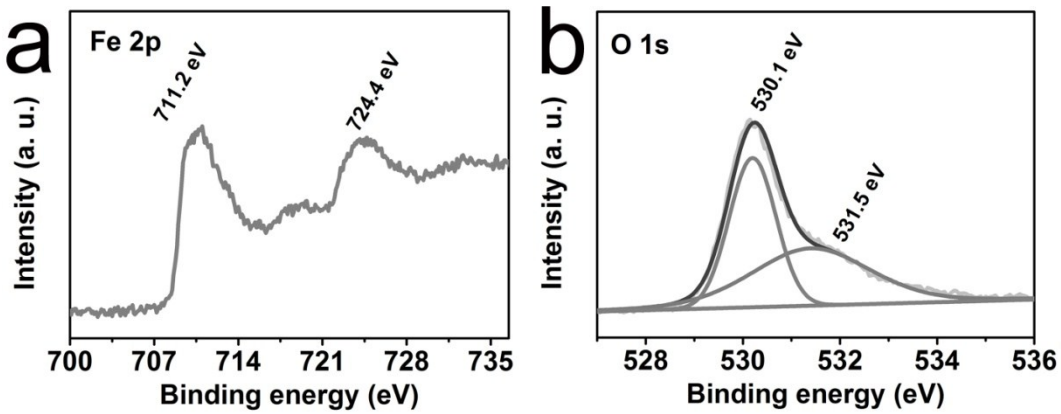

Fig. S3. XPS spectra of Fe_2O_3 in the (a) Fe 2p and (b) O 1s regions.

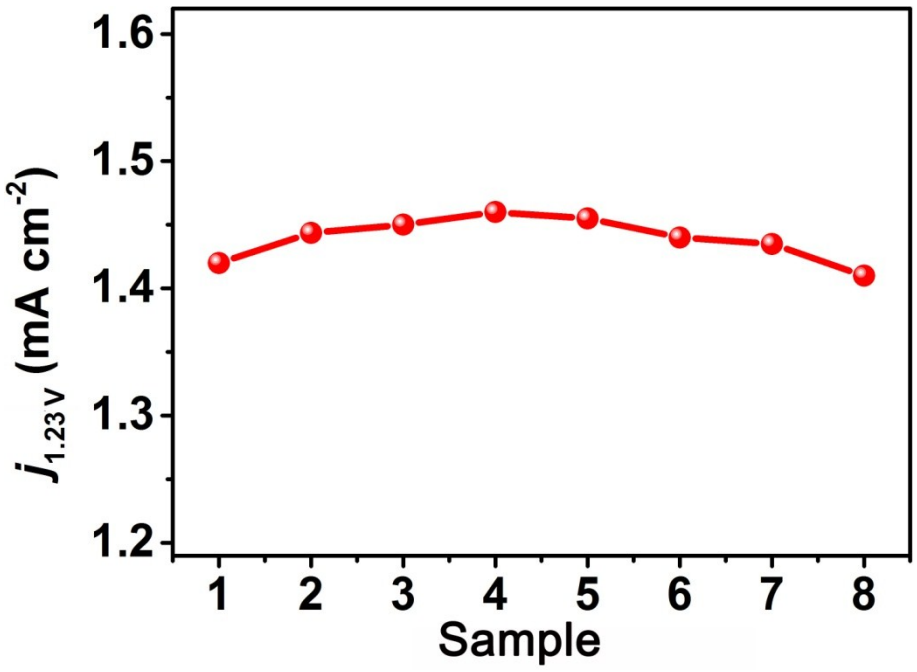

Fig. S4. Photocurrent densities of Se-Fe_2O_3 samples at 1.23 V vs. RHE.

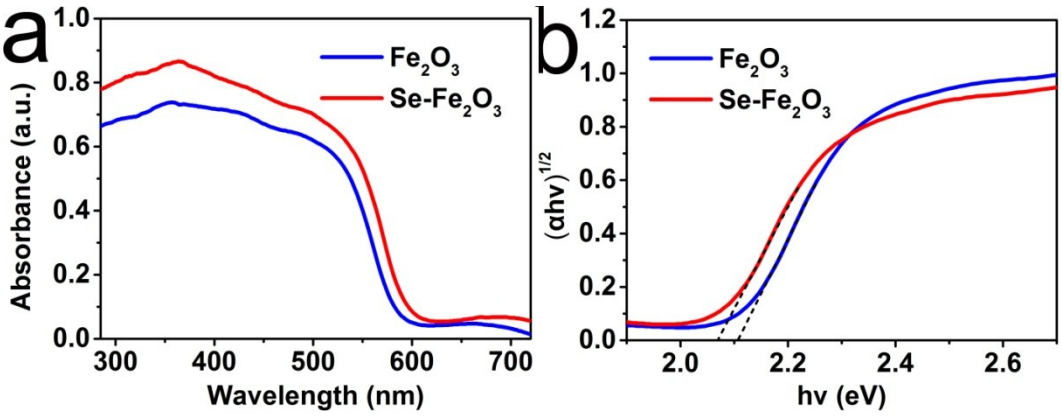

Fig. S5. (a) UV-visible absorption spectra and (b) Tauc plots of Fe_2O_3 and Se-Fe_2O_3.

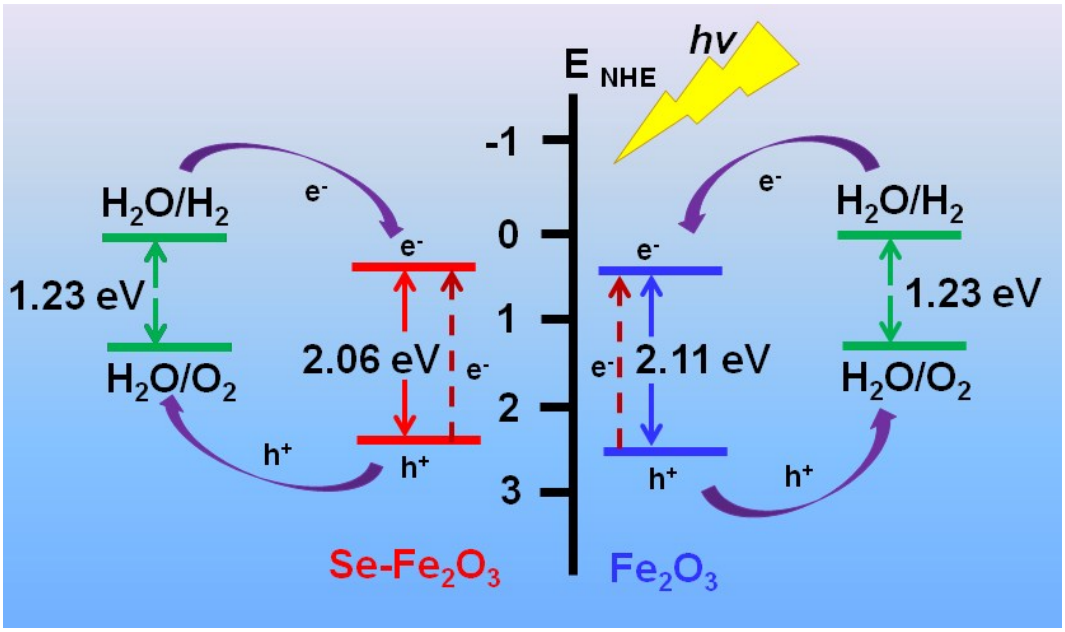

Fig. S6. Energy diagram of Fe_2O_3 and Se-Fe_2O_3.

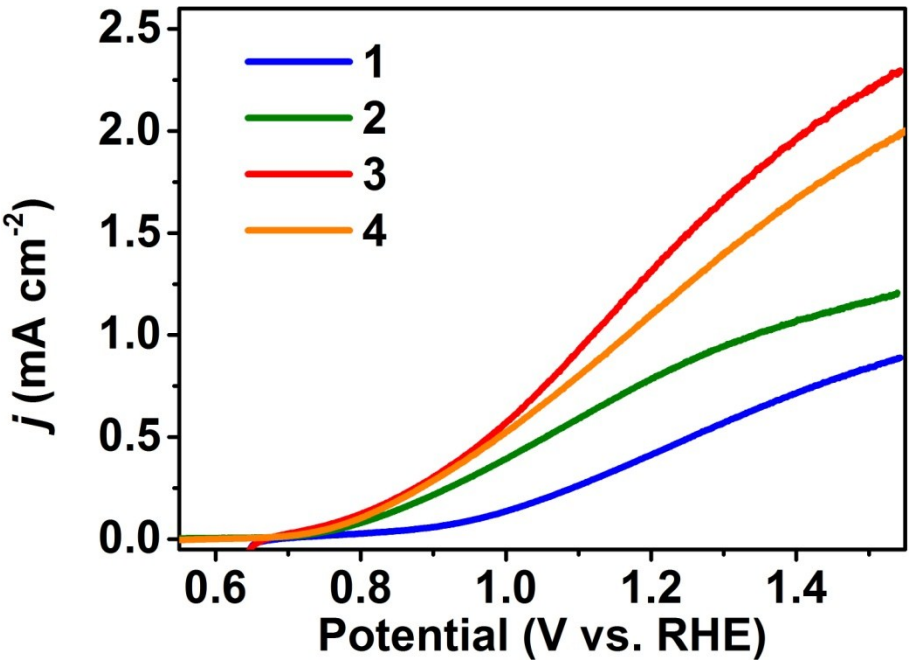

Fig. S7. LSV curves of Se doped Fe_2O_3 with different Se doping degrees: 0 (curve 1), 3.11% (curve 2), 5.06% (curve 3), and 8.67% (curve 4).

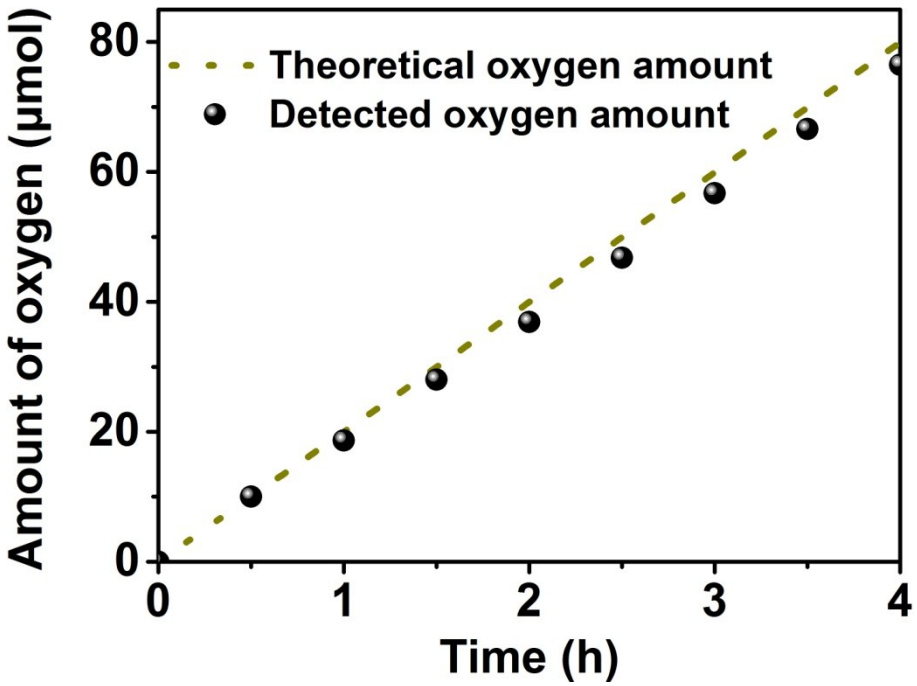

Fig. S8. Time-dependent oxygen evolution of Se-Fe_2O_3 at 1.23 V vs. RHE in 1.0 M NaOH.

Table S1. Comparison of doped Fe_2O_3 photoanodes in PEC system.

Photoanode	***j* at 1.23 V vs. RHE (mA cm^{-2})**	**Potoconversion efficiency (%)**	**Ref.**
Se-Fe_2O_3	1.44	14	This work
Sn,Zr-Fe_2O_3	1.34	14	1
Mn:Fe_2O_3	1.60	12	2
Si doped α-Fe_2O_3	1.45	–	3
La doped hematite	0.11	–	4
Ti doped hematite	0.42	–	5
Sn-doped α-Fe_2O_3	1.00	–	6
Sn,Be-doped α-Fe_2O_3	1.70	–	
Sn-doped hematite	1.86	–	7
Grad-P:Fe_2O_3	1.48	22	8
Pt-doped α-Fe_2O_3	~0.70	–	9
Ge-doped α-Fe_2O_3	1.40	–	10

References

1 A. G. Tamirat, W.-N. Su, A. A. Dubale, H.-M. Chena and B.-J. Hwang, *J. Mater. Chem. A,* 2015, **3**, 5949-5961.

2 J. Huang, G. Hu, Y. Ding, M. Pang and B. Ma, *J. Catal.,* 2016, **340**, 261-269.

3 I. Cesar, A. Kay, J. A. G. Martinez and M. Grätzel, *J. Am. Chem. Soc.,* 2006, **128**, 4582-4583.

4 N. Li, S. Jayaraman, S. Y. Tee, P. S. Kumar, C. J. J. Lee, S. L. Liew, D. Chi, T. S. A. Hor, S. Ramakrishna and H.-K. Luo, *J. Mater. Chem. A,* 2014, **2**, 19290-19297.

5 D. Yan, J. Tao, K. Kisslinger, J. Cen, Q. Wu, A. Orlovb and M. Liu, *Nanoscale,* 2015, **7**, 18515-18523.

6 A. Annamalai, H. H. Lee, S. H. Choi, S. Y. Lee, E. Gracia-Espino, A.Subramanian, J. Park, K. Kong and J. S. Jang, *Sci. Rep.,* 2016, **6**, 28183.

7 Y. Ling, G. Wang, D. A. Wheeler, J. Z. Zhang and Y. Li, *Nano Lett.,* 2011, **11**, 2119-2125.

8 Z. Luo, C. Li, S. Liu, T. Wang and J. Gong, *Chem. Sci.,* 2017, **8**, 91-100.

9 Y. Hu, A. Kleiman-Shwarsctein, A.J. Forman, D. Dazen, J. N. Park and E. W. McFarland, *Chem. Mater.,* 2008, **20***,* 3803-3805.

10 J. Liu, Y. Y. Cai, Z. F. Tian, G. S. Ruan, Y. X. Ye, C. H. Liang, G. S. Shao, *Nano Energy,* 2014, **9**, 282-290.